

Numerical study of flow generated in a lake and experiment using GPS

Ying Liu¹

Kazuhiro Yamamoto²

Majda Ceric³

Masaji Watanabe⁴

(Received 15 August 2008; revised 01 April 2009)

Abstract

A finite element method is applied to a system of partial differential equations governing the dynamics of flow in order to study currents generated in a lake. Experiments using a float equipped with a GPS unit calibrate and validate the numerical results.

Contents

1	Introduction	C913
2	Finite element method for analyzing flow in the Kojima Lake	C915
2.1	Governing equations of flow	C915
2.2	Finite element discretization	C916
2.3	Time step approximation	C919

<http://anziamj.austms.org.au/ojs/index.php/ANZIAMJ/article/view/1470>
gives this article, © Austral. Mathematical Soc. 2009. Published June 12, 2009. ISSN 1446-8735. (Print two pages per sheet of paper.)

<i>1 Introduction</i>	C913
3 Experiment using the GPS-float and simulation of its motion	C921
4 Discussion	C927
References	C928

1 Introduction

The bank isolating Kojima Lake has six gates, which are opened when necessary to discharge water to Kojima Bay in order to lower the lake's water level [5]. In such an event, a current is generated in Kojima Lake. On May 31, 2008, those gates were opened from 2:36 to 5:49 AM GMT. Figure 1 shows the change of the water levels of the Kojima Lake, the Kurashiki river, the Sasagase river and Kojima Bay during that period. These data were introduced into a finite element analysis of momentum equations and a continuity equation. We took the upwind type technique in the weighted averaged approximation in time discretization to account for convection terms. In previous work [5] the convex profile of vertical distribution of horizontal velocities was obtained. In this work we show that it is possible for the vertical distribution to have concave structure. Note that the water level of the lake decreased by approximately 0.45 m during the period the gates were opened on May 31, 2008.

The driving force of the GPS-float is the fluid resistance on the pair of rectangular plates attached underneath the water surface. While the GPS-float travels on the surface, a GPS unit evaluates its position consecutively, and temporal and spatial data to track the float are transmitted to be recorded. On the other hand, the fluid resistance on the plates is represented in terms of the velocity of flow. Once the fluid resistance is specified, the motion of the GPS-float is simulated by solving its momentum equations, and a numerical result and an experimental result compared. The technique determines the

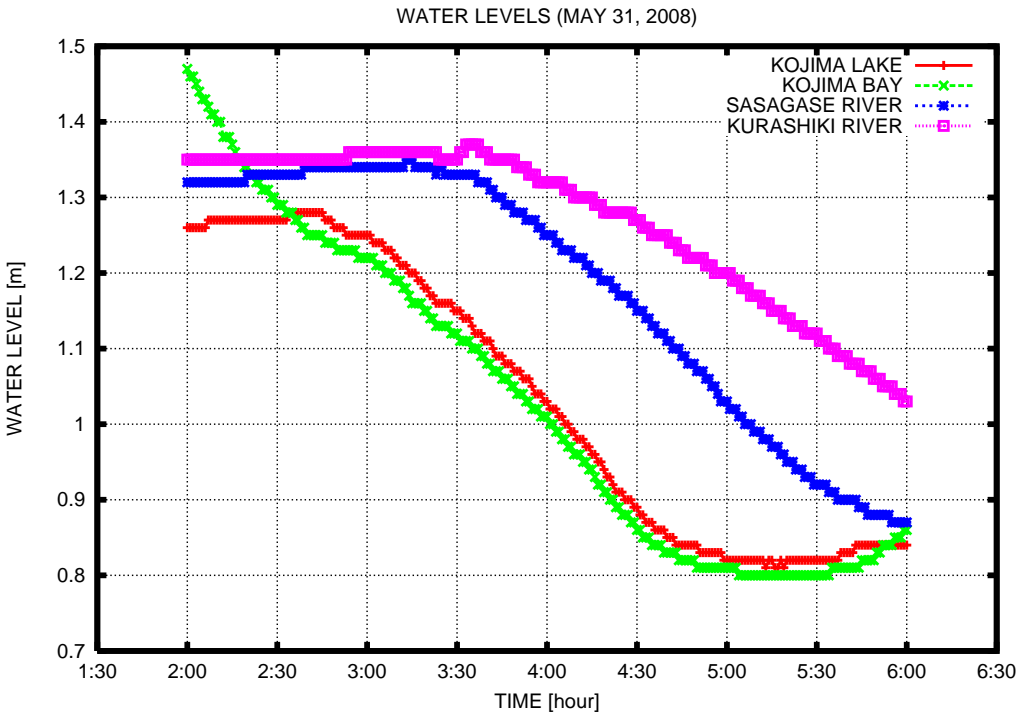


FIGURE 1: Change of water levels on May 31, 2008.

horizontal components of velocity and their vertical distribution.

The numerical result and the experimental result from May 31, 2008 were compared in order to check the validity of the numerical result. Data from Oct 23, 2004 were tested against data from May 31, 2008 in order to see how different final boundary conditions, as well as different equation parameters, affect the final result.

2 Finite element method for analyzing flow in the Kojima Lake

2.1 Governing equations of flow

We analyze here a finite element method to solve a series of differential equations governing shallow water equations (1), (2), (3) [1, 2, 3]:

$$\frac{\partial M}{\partial t} + u \frac{\partial M}{\partial x} + v \frac{\partial M}{\partial y} = -g(h + \zeta) \frac{\partial \zeta}{\partial x} + A_h \left(\frac{\partial^2 M}{\partial x^2} + \frac{\partial^2 M}{\partial y^2} \right) - \frac{\tau_x}{\rho_0}, \quad (1)$$

$$\frac{\partial N}{\partial t} + u \frac{\partial N}{\partial x} + v \frac{\partial N}{\partial y} = -g(h + \zeta) \frac{\partial \zeta}{\partial y} + A_h \left(\frac{\partial^2 N}{\partial x^2} + \frac{\partial^2 N}{\partial y^2} \right) - \frac{\tau_y}{\rho_0}, \quad (2)$$

$$\frac{\partial \zeta}{\partial t} + \frac{\partial M}{\partial x} + \frac{\partial N}{\partial y} = 0, \quad (3)$$

where surface stresses

$$\tau_x = \frac{\rho_0 \gamma^2 \sqrt{M^2 + N^2}}{(h + \zeta)^2} M, \quad \tau_y = \frac{\rho_0 \gamma^2 \sqrt{M^2 + N^2}}{(h + \zeta)^2} N, \quad (4)$$

parameter $\gamma^2 = 0.0026$ is the bottom friction coefficient [6], $h \equiv h(x, y)$ is the bottom topography, $z = \zeta(x, y)$ is the lake surface height, and water fluxes M and N are obtained by integrating the x -component and the y -component

of the velocity over the depth, respectively:

$$M = \int_{-h}^{\zeta} u \, dz, \quad N = \int_{-h}^{\zeta} v \, dz. \quad (5)$$

A_h is a constant that represents eddy viscosity, whereas $\rho_0 = 1000 \text{ kg/m}^3$ is the constant density of water. We set $A_h = 0.001$ for the result obtained on May 31, 2008, and $A_h = 0.01$ for the result obtained on Oct 23, 2004.

Along the curve

$$\frac{dx}{dt} = u, \quad \frac{dy}{dt} = v,$$

equations (1) and (2) become

$$\frac{dM}{dt} = -g(h + \zeta) \frac{\partial \zeta}{\partial x} + A_h \left(\frac{\partial^2 M}{\partial x^2} + \frac{\partial^2 M}{\partial y^2} \right) - \frac{\tau_x}{\rho_0}, \quad (6)$$

$$\frac{dN}{dt} = -g(h + \zeta) \frac{\partial \zeta}{\partial y} + A_h \left(\frac{\partial^2 N}{\partial x^2} + \frac{\partial^2 N}{\partial y^2} \right) - \frac{\tau_y}{\rho_0}. \quad (7)$$

2.2 Finite element discretization

After multiplying the equation (6) by δM and applying Green's theorem, we integrate it over a domain Ω . Thus we obtain [7]

$$\begin{aligned} \iint_{\Omega} \delta M \frac{\partial M}{\partial t} \, dx \, dy &= -g \iint_{\Omega} \delta M (h + \zeta) \frac{\partial \zeta}{\partial x} \, dx \, dy \\ &\quad - A_h \iint_{\Omega} \left(\frac{\partial \delta M}{\partial x} \frac{\partial M}{\partial x} + \frac{\partial \delta M}{\partial y} \frac{\partial M}{\partial y} \right) \, dx \, dy \\ &\quad + A_h \int_{\Gamma} \delta M \left(-\frac{\partial M}{\partial y} \, dx + \frac{\partial M}{\partial x} \, dy \right) \\ &\quad - \frac{1}{\rho_0} \iint_{\Omega} \delta M \tau_x \, dx \, dy. \end{aligned} \quad (8)$$

Under appropriate boundary conditions, we set

$$\int_{\Gamma} \delta M \left(-\frac{\partial M}{\partial y} dx + \frac{\partial M}{\partial x} dy \right) = 0. \tag{9}$$

Let the boundary Γ be a disjoint union of the rigid boundary Γ_1 and the open boundary Γ_2 . Furthermore, δM is an arbitrary function that vanishes along the rigid boundary Γ_1 . Then the left-hand side of the equation (9) is

$$\begin{aligned} & \int_{\Gamma} \delta M \left(-\frac{\partial M}{\partial y} dx + \frac{\partial M}{\partial x} dy \right) \\ = & \int_{\Gamma_1} \delta M \left(-\frac{\partial M}{\partial y} dx + \frac{\partial M}{\partial x} dy \right) + \int_{\Gamma_2} \delta M \left(-\frac{\partial M}{\partial y} dx + \frac{\partial M}{\partial x} dy \right) \\ = & \int_{\Gamma_2} \delta M (dy, -dx) \cdot \nabla M ds, \end{aligned} \tag{10}$$

where s parametrises boundary Γ_2 . We assume that a uniform flow is formed at an open boundary perpendicular to a long channel such as cross sections of rivers and gate ends. Thus the Neumann condition

$$\frac{\partial M}{\partial n} = \frac{\partial M}{\partial x} dy - \frac{\partial M}{\partial y} dx = (dy, -dx) \cdot \nabla M = 0 \tag{11}$$

holds on Γ_2 . Decompose fields

$$\begin{aligned} M &= \sum_{j=1}^n \phi_j M_j, & N &= \sum_{j=1}^n \phi_j N_j, \\ h &= \sum_{j=1}^n \phi_j h_j, & \zeta &= \sum_{j=1}^n \phi_j \zeta_j, \\ \delta M &= \phi_i, \end{aligned} \tag{12}$$

where $\phi_1, \phi_2, \dots, \phi_n$ are basis functions, n is the number of nodes, $i, j, k = 1, 2, \dots, n$. Now, when we substitute (12) into the equation (8), using equation (9), we write [7]

$$\sum_j \frac{\partial M_j}{\partial t} \iint_{\Omega} \phi_i \phi_j dx dy$$

$$\begin{aligned}
 &= -g \sum_j \zeta_j \iint_{\Omega} \sum_k (h_k \phi_k + \zeta_k \phi_k) \phi_i \frac{\partial \phi_j}{\partial x} dx dy \\
 &\quad - A_h \sum_j M_j \iint_{\Omega} \left(\frac{\partial \phi_i}{\partial x} \frac{\partial \phi_j}{\partial x} + \frac{\partial \phi_i}{\partial y} \frac{\partial \phi_j}{\partial y} \right) dx dy \\
 &\quad - \gamma^2 \sum_j M_j \iint_{\Omega} \frac{\sqrt{\sum_k (M_k \phi_k)^2 + \sum_k (N_k \phi_k)^2}}{\sum_k (h_k \phi_k + \zeta_k \phi_k)^2} \phi_i \phi_j dx dy .
 \end{aligned} \tag{13}$$

In the same way we obtain an equation for N. For the continuity equation (3), we write

$$\begin{aligned}
 &\sum_j \frac{\partial \zeta_j}{\partial t} \iint_{\Omega} \phi_i \phi_j dx dy + \sum_j M_j \iint_{\Omega} \phi_i \frac{\partial \phi_j}{\partial x} dx dy \\
 &\quad + \sum_j N_j \iint_{\Omega} \phi_i \frac{\partial \phi_j}{\partial y} dx dy = 0 .
 \end{aligned}$$

When the integration is carried out in each element, $\sum_k M_k \phi_k$, $\sum_k N_k \phi_k$, $\sum_k h_k \phi_k$ and $\sum_k \zeta_k \phi_k$ are replaced with their averages over the element \bar{M}_{Δ} , \bar{N}_{Δ} , \bar{h}_{Δ} and $\bar{\zeta}_{\Delta}$. The momentum equation (13) becomes [7]

$$\begin{aligned}
 \frac{\partial M_j}{\partial t} \iint_{\Delta} \phi_i \phi_j dx dy &= -g \zeta_j (\bar{h}_{\Delta} + \bar{\zeta}_{\Delta}) \iint_{\Delta} \phi_i \frac{\partial \phi_j}{\partial x} dx dy \\
 &\quad - A_h M_j \iint_{\Delta} \left(\frac{\partial \phi_i}{\partial x} \frac{\partial \phi_j}{\partial x} + \frac{\partial \phi_i}{\partial y} \frac{\partial \phi_j}{\partial y} \right) dx dy \\
 &\quad - \gamma^2 \frac{\sqrt{\bar{M}_{\Delta}^2 + \bar{N}_{\Delta}^2}}{(\bar{h}_{\Delta} + \bar{\zeta}_{\Delta})^2} M_j \iint_{\Delta} \phi_i \phi_j dx dy .
 \end{aligned}$$

The equation for N is obtained in the same way. The continuity equation (14) becomes

$$\frac{\partial \zeta_j}{\partial t} \iint_{\Delta} \phi_i \phi_j dx dy + M_j \iint_{\Delta} \phi_i \frac{\partial \phi_j}{\partial x} dx dy + N_j \iint_{\Delta} \phi_i \frac{\partial \phi_j}{\partial y} dx dy = 0 .$$

Let

$$A_{ij} = \sum_e \iint_{\Delta} \phi_i \phi_j \, dx \, dy, \quad (14)$$

$$A'_{ij} = \gamma^2 \sum_e \frac{\sqrt{\bar{M}_{\Delta_e}^2 + \bar{N}_{\Delta_e}^2}}{(\bar{h}_{\Delta_e} + \bar{\zeta}_{\Delta_e})^2} A_{ij}, \quad (15)$$

$$B_{ij} = \sum_e \iint_{\Delta} \phi_i \frac{\partial \phi_j}{\partial x} \, dx \, dy, \quad (16)$$

$$B'_{ij} = g \sum_e (\bar{h}_{\Delta_e} + \bar{\zeta}_{\Delta_e}) B_{ij}, \quad (17)$$

$$C_{ij} = \sum_e \iint_{\Delta} \phi_i \frac{\partial \phi_j}{\partial y} \, dx \, dy, \quad (18)$$

$$D_{ij} = A_h \sum_e \iint_{\Delta} \left(\frac{\partial \phi_i}{\partial x} \frac{\partial \phi_j}{\partial x} + \frac{\partial \phi_i}{\partial y} \frac{\partial \phi_j}{\partial y} \right) dx \, dy, \quad (19)$$

where ne is the number of elements consisted in Ω and $e = 1, 2, \dots, ne$.

2.3 Time step approximation

For a given ζ_j^l, M_j^l and N_j^l , ζ_j^{l+1} can be calculated. The continuity equation (14) then becomes

$$A_{ij} \zeta_j^{l+1} = -\Delta t (B_{ij} M_j^l + C_{ij} N_j^l) + A_{ij} \zeta_j^l. \quad (20)$$

Putting $-\Delta t (B_{ij} M_j^l + C_{ij} N_j^l) + A_{ij} \zeta_j^l = p_{3i}$ and $A_{3ij} = A_{ij}$, we write

$$A_3 \zeta^{l+1} = p_3. \quad (21)$$

For given values of M_j^l, N_j^l, ζ_j^l and ζ_j^{l+1} , we calculate the values of M_j^{l+1} and N_j^{l+1} . The momentum equation (14) then becomes

$$\sum_j A_{ij} \frac{M_j^{l+1} - M_j^l}{\Delta t} = - \sum_j \{ B'_{ij} [(1 - \theta) \zeta_j^l + \theta \zeta_j^{l+1}]$$

$$+ D_{ij} [(1 - \theta) M_j^l + \theta M_j^{l+1}] + A'_{ij} M_j^l \},$$

where θ is a parameter that appears in the weighted averaged approximation in time discretization. The previous equation is written as

$$\begin{aligned} \sum_j (A_{ij} + \theta D_{ij}) M_j^{l+1} = -\Delta t \sum_j \{ [A'_{ij} + (1 - \theta) D_{ij}] M_j^l \\ + B'_{ij} [(1 - \theta) \zeta_{j*}^l + \theta \zeta_j^{l+1}] \} + \sum_j A_{ij} M_j^l. \end{aligned} \quad (22)$$

Instead of calculating ζ_j^l , we calculate ζ_{j*}^l at the point (x^*, y^*) , where x^* and y^* are calculated from the system of ordinary differential equations

$$\frac{dx}{dt} = u, \quad \frac{dy}{dt} = v. \quad (23)$$

Thus,

$$x^* = x_j - \frac{M_j^l}{\zeta_j^l + h_j} \Delta t, \quad y^* = y_j - \frac{N_j^l}{\zeta_j^l + h_j} \Delta t. \quad (24)$$

Denoting the right-hand side of equation (22) by p_{1i} and $\sum_j (A_{ij} + \theta D_{ij}) = A_{1ij}$, then M_j^{l+1} is the solution of the simultaneous linear equation

$$A_1 M^{l+1} = p_1. \quad (25)$$

We similarly obtain an equation for N :

$$A_2 N^{l+1} = p_2. \quad (26)$$

Let a_{ij} be the entry in the i th row and the j th column of A_1 . Suppose that the i th node is on the rigid boundary. We redefine $a_{ij} = \delta_{ij}$, and set the i th entry of p_1 to 0. For given values of $M_j^l, M_j^{l+1}, N_j^l, N_j^{l+1}$ and ζ_j^l, ζ_j^{l+1} is found. The continuity equation (20) becomes

$$\sum_j A_{ij} \zeta_j^{l+1} = -\Delta t \sum_j \{ B_{ij} [(1 - \theta) M_j^l + \theta M_j^{l+1}]$$

$$+ C_{ij} [(1 - \theta) N_j^l + \theta N_j^{l+1}] \} + \sum_j A_{ij} \zeta_j^l. \quad (27)$$

Denoting the right-hand side of the above equation by p'_3 , then ζ_j^{l+1} is the solution of the simultaneous linear equation

$$A_3 \zeta^{l+1} = p'_3. \quad (28)$$

Let a_{ij} be the entry in the i th row and the j th column of A_3 . Suppose that the i th node is on the open boundary. We redefine $a_{ij} = \delta_{ij}$, and set the i th entry of p_3 to the value of ζ_i^{l+1} given by the boundary conditions (Figure 1). At the rigid boundaries the values of M and N are set to zero. Initial conditions are given as $M = 0$ and $N = 0$ at all node points.

The finite element method was applied to equations (1), (2) and (3) to simulate the flow generated in the Kojima Lake. The finite element mesh consisting of 2232 elements and 1246 nodes in the entire region and in a region near the gates is used [5]. Figure 2 shows numerically calculated velocity vectors at 80 minutes after the gates were opened on May 31, 2008, in the entire region and in a region near the gates.

3 Experiment using the GPS-float and simulation of its motion

A GPS-float [5] was used in an experiment of flow generated in Kojima Lake on May 31, 2008 on Kojima Lake. Its position is recorded every second between 3:37 and 5:29 AM GMT. During that period, the GPS-float traveled over the distance of 1211.75 m with average velocity of approximately 0.180777 m/s. On Oct 23, 2004 the GPS-float was used in an experiment from 2:35 to 3:40 AM GMT when it traveled over the distance of 631.219 m. On that day the GPS-float traveled with the average velocity of approximately 0.161976 m/s.

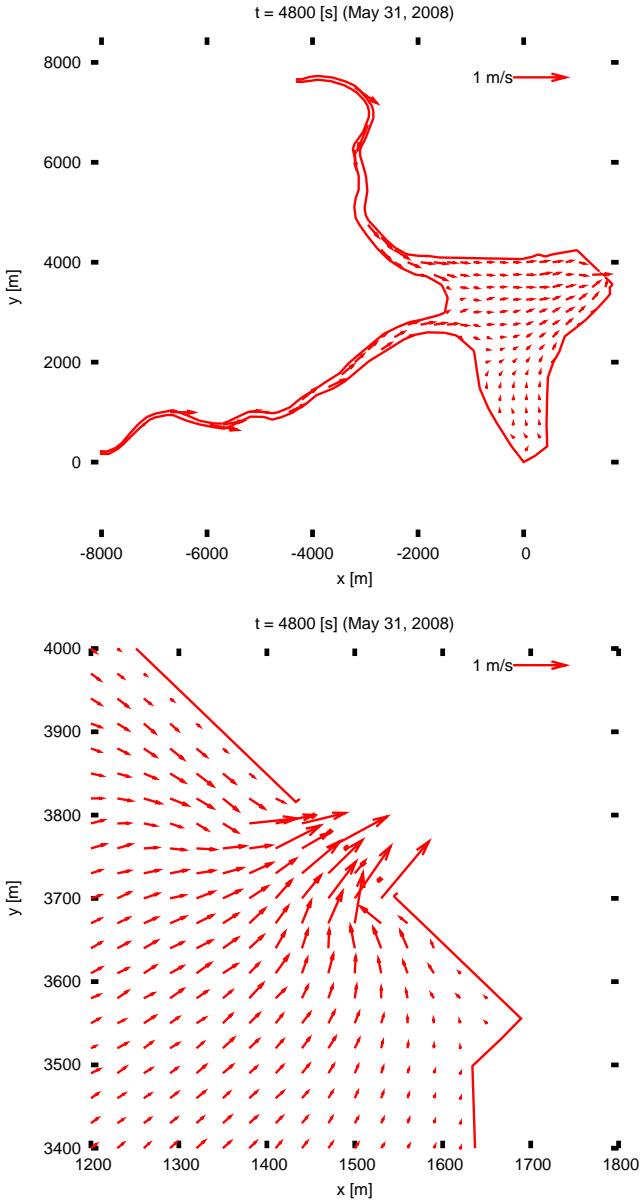


FIGURE 2: Velocity vectors in the entire region and in a region near the gates at time $t = 4800$ s after the gates were opened on May 31, 2008.

The vertical average of the velocity components $\mathbf{u}(x, y, z, t)$ and $\mathbf{v}(x, y, z, t)$ should equal to $\bar{\mathbf{u}}(x, y, t)$ and $\bar{\mathbf{v}}(x, y, t)$. They should also vanish at $z = -h(x, y)$. We assume the functional form

$$\mathbf{u}(x, y, z, t) = c\{z + h(x, y)\}^\alpha \bar{\mathbf{u}}(x, y, t), \quad (29)$$

that vanishes for $z = -h(x, y)$. Integrating it from $-h(x, y)$ to $\zeta(x, y, t)$ we obtain

$$(\zeta + h) \bar{\mathbf{u}} = \int_{-h}^{\zeta} \mathbf{u} \, dz = c \bar{\mathbf{u}} \frac{(\zeta + h)^{\alpha+1}}{\alpha + 1}, \quad (30)$$

which leads to

$$c = \frac{\alpha + 1}{(\zeta + h)^\alpha}. \quad (31)$$

These assumptions lead to the following expression for velocities $\mathbf{u}(x, y, z, t)$ and $\mathbf{v}(x, y, z, t)$ in terms of $\bar{\mathbf{u}}(x, y, t)$ and $\bar{\mathbf{v}}(x, y, t)$ [5]:

$$\begin{aligned} \mathbf{u}(x, y, z, t) &= (\alpha + 1) \left(\frac{z + h(x, y)}{\zeta(x, y, t) + h(x, y)} \right)^\alpha \bar{\mathbf{u}}(x, y, t) \\ \mathbf{v}(x, y, z, t) &= (\alpha + 1) \left(\frac{z + h(x, y)}{\zeta(x, y, t) + h(x, y)} \right)^\alpha \bar{\mathbf{v}}(x, y, t). \end{aligned} \quad (32)$$

Here $\bar{\mathbf{u}}$ and $\bar{\mathbf{v}}$ are the vertically averaged velocity components:

$$\bar{\mathbf{u}} = \frac{1}{\zeta(x, y, t) + h(x, y)} \mathbf{M}(x, y, t), \quad \bar{\mathbf{v}} = \frac{1}{\zeta(x, y, t) + h(x, y)} \mathbf{N}(x, y, t), \quad (33)$$

where \mathbf{M} and \mathbf{N} are given by equation (5). The system of equations (32) is solved for α equal to 0.1 and 0.2, and the results are shown in Figures 3 and 4. This system of equations is solved by introducing data from May 31, 2008 and Oct 23, 2004. The motion of the GPS-float is simulated by solving its momentum equations [4, 5].

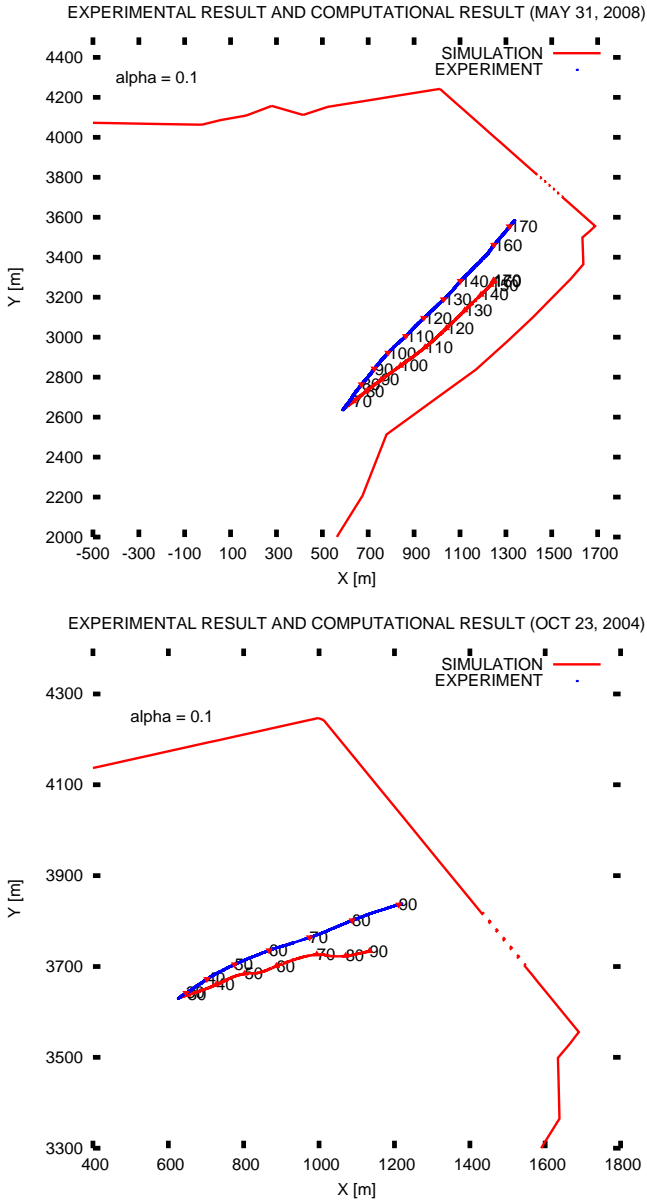


FIGURE 3: Trajectory of the GPS-float with elapsed time in minutes shown along side the path for $\alpha = 0.1$ on May 31, 2008 and Oct 23, 2004 respectively.

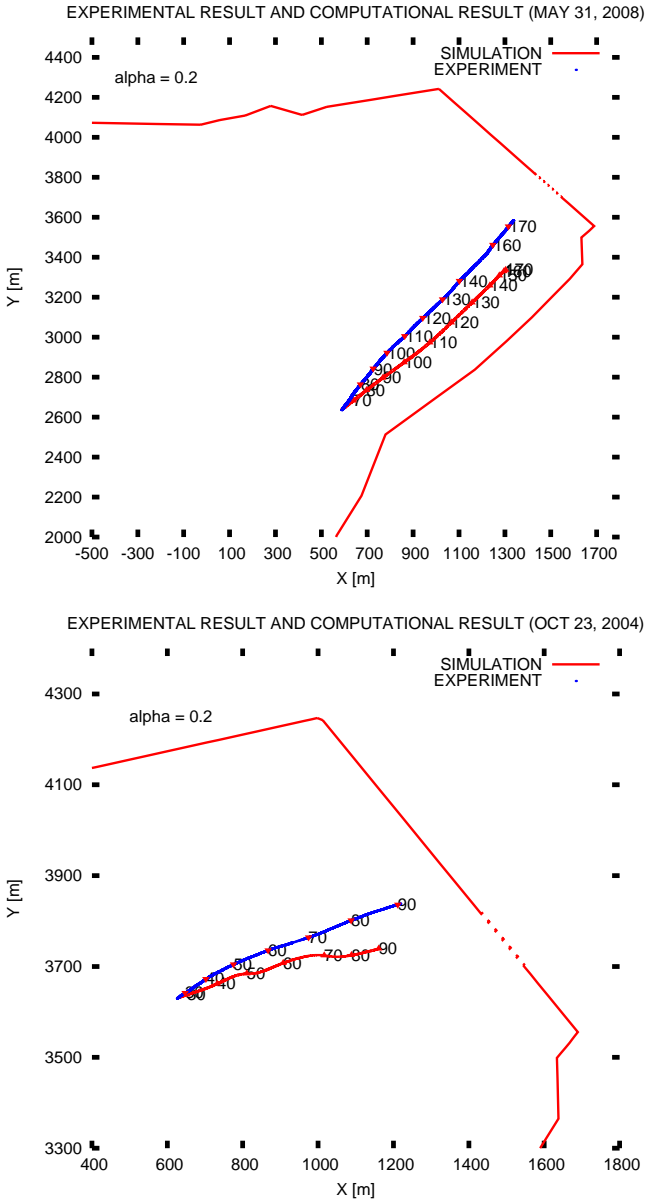


FIGURE 4: Trajectory of the GPS-float with elapsed time in minutes shown along side the path for $\alpha = 0.2$ on May 31, 2008 and Oct 23, 2004 respectively.

TABLE 1: Total difference between the numerical and experimental results at every 10 minutes after starting the GPS-float experiment on Oct 23, 2004. Values in the table are given in metres.

α	$d(m=1)$	$d(m=2)$	$d(m=3)$	$d(m=4)$	$d(m=5)$	$d(m=6)$
0.1	17.95	50.37	89.54	129.65	191.22	298.76
0.2	20.48	58.77	103.72	159.69	226.30	322.88

TABLE 2: Total difference between the numerical and experimental results at every 10 minutes after starting the GPS-float experiment on May 31, 2008. Values in the table are given in metres.

α	$d(m=1)$	$d(m=2)$	$d(m=3)$	$d(m=4)$	$d(m=5)$	$d(m=6)$
0.1	27.42	79.96	158.16	255.38	367.35	477.33
0.2	27.26	77.90	157.26	264.36	390.03	519.05

The parameter d in Tables 1 and 2 is

$$d = \sum_{i=1}^m d_i,$$

where $m = 1, 2, \dots, 6$. The parameter

$$d_i = \sqrt{(x_{e_i} - x_{s_i})^2 + (y_{e_i} - y_{s_i})^2},$$

where $i = 1, 2, \dots, 6$. Furthermore, (x_{e_i}, y_{e_i}) is the experimentally obtained position of the GPS-float, whereas (x_{s_i}, y_{s_i}) is the numerically calculated position of the GPS-float, 10–60 minutes after starting the experiment.

4 Discussion

Figures 3 and 4 show experimental and numerical results of the GPS-float's motion. Those figures are generated for different values of the vertical profile exponent α , in order to find a numerical result that is closest to the experimental one. On May 31, 2008 the best numerical result is generated for $\alpha = 0.1$ (Table 2). On Oct 23, 2004 the best numerical result is generated for the same value of $\alpha = 0.1$ (Table 1). From the system of equations (32), α is directly proportional to the vertical average of the velocity components $\mathbf{u}(x, \mathbf{y}, z, t)$ and $\mathbf{v}(x, \mathbf{y}, z, t)$, which are denoted by $\bar{\mathbf{u}}(x, \mathbf{y}, t)$ and $\bar{\mathbf{v}}(x, \mathbf{y}, t)$.

The initial water levels of Kojima Lake, Kojima Bay, Kurashiki river and Sasagase river, that are used as boundary conditions are different on May 31, 2008 and Oct 23, 2004. Topographical data are the same. Those data are introduced into computational analysis of currents generated in Kojima Lake.

Acknowledgements The authors are grateful for the help of those people in the Kojima Bay Central Administration Office, the Section of Land Improvement in the Kojima Bay Area, those people in the Okayama Prefecture Okayama Development Bureau, those people in the Machining Center, the Faculty of Engineering, Okayama University, and those people in the Chugoku–Shikoku Agricultural Administration Office. Authors are also grateful for the help of those people who assisted with the experiments, the measurements, and the analyses. The information for generating the figures concerning the Kojima Lake is partially based on maps © Shobunsha Publications, INC., © Nihon Computer Graphic CO., LTD. This work was based on results in a Trust Research commissioned by Chugoku–Shikoku Agricultural Administration Office, and was supported in part by JSPS MEXT Grant-in-Aid for Scientific Research (B) (16380161).

References

- [1] O. C. Zienkiewicz and R. L. Taylor, *The finite Element Method*, Volume 3, Fluid Dynamics, Fifth Edition, Butterworth–Heinemann, Oxford, 2000 (First published in 1967 by McGraw–Hill). **C915**
- [2] R. G. Dean and R. A. Dalrymple, *Water Wave Mechanics for Engineers and Scientists*, Advanced Series on Ocean Engineering, Volume 2, World Scientific, Singapore, 1991 (First published in 1984 by Prentice Hall, INC., Reprinted in 1992, 1993, 1994, 1995, 1998). **C915**
- [3] J. Matsumoto, *Water Environmental Engineering*, Asakura Publishing Company, Tokyo, 1994 (In Japanese). **C915**
- [4] M. Watanabe, Mathematical model and numerical simulation for motion of the GPS-float in study of currents in water environment, *International Journal of Pure and Applied Mathematics*, **14** (3) (2004) 377–395. **C923**
- [5] S. Sumida, Y. Liu, Y. Li, K. Yamamoto, M. Ceric, M. Watanabe, Numerical study of currents generated in a lake and verification by experiment, *ANZIAM J.*, **49** (EMAC2007) pp. C541–C558, 2008. <http://anziamj.austms.org.au/ojs/index.php/ANZIAMJ/issue/view/13> **C913**, **C921**, **C923**
- [6] Yoshiaki Iwasa, *Engineering Limnology*, Sankaido Publishing Co., Ltd., 1990 (In Japanese) **C915**
- [7] Masaji Watanabe, A Numerical Simulation of Lake Flow and a GPS-Float Experiment, The Second International Symposium on Water Environment, Okayama University, September 13–14, 1999, *Journal of the Faculty of Environmental Science and Technology, Okayama University* (Special Edition), pp. 111–116. **C916**, **C917**, **C918**

Author addresses

1. **Ying Liu**, Graduate School of Environmental Science, Okayama University, JAPAN.
2. **Kazuhiro Yamamoto**, Graduate School of Environmental Science, Okayama University, JAPAN.
3. **Majda Ceric**, Graduate School of Environmental Science, Okayama University, JAPAN.
4. **Masaji Watanabe**, Graduate School of Environmental Science, Okayama University, JAPAN.
<mailto:watanabe@ems.okayama-u.ac.jp>